Available online at www.sciencedirect.com

ScienceDirect

www.elsevier.com/locate/jes

JES JOURNAL OF ENVIRONMENTAL SCIENCES

www.jesc.ac.cn

Effect of Ni–V loading on the performance of hollow anatase TiO_2 in the catalytic combustion of dichloromethane

Bing Zhou[1], *Xixiong Zhang*[2], *Yong Wang*[1], *Jing Xie*[1], *Kang Xi*[1], *Ying Zhou*[1], *Hanfeng Lu*[1,*]

1. *College of Chemical Engineering, Institute of Catalytic Reaction Engineering, Zhejiang University of Technology, Hangzhou 310014, China*
2. *College of Environment, Zhejiang University of Technology, Hangzhou 310014, China*

ARTICLE INFO

Article history:
Received 30 November 2018
Revised 7 April 2019
Accepted 12 April 2019
Available online 25 April 2019

Keywords:
Catalytic combustion
Dichloromethane (DCM)
TiO_2 catalyst
Ni–V/TiO_2 catalyst

ABSTRACT

A catalyst based on mixed V-Ni oxides supported on TiO_2 (Ni–V/TiO_2) was obtained using the sol–gel method. Its catalytic performance relative to dichloromethane (DCM) degradation was investigated. Characterization and analysis were conducted using transmission electron microscopy, H_2 temperature-programmed reduction, pyridine–Fourier transform infrared spectroscopy (FTIR) characterization, and X-ray diffraction. Results showed that the original hollow anatase structure of pure TiO_2 was well-maintained after Ni–V loading. The loading of NiO–VO_x not only significantly improved the stability of pure TiO_2 but also inhibited the formation of the by-product monochloromethane (MCM). Among the series of Ni–V/TiO_2 catalysts, 4%Ni–V/TiO_2 possessed the highest catalytic activity, with 90% DCM conversion at only 203°C. No by-products and no significant changes in the catalytic activity were observed during combustion of DCM after 100 hr of a continuous stability test. Furthermore, thermogravimetric analysis (O_2-TG) and energy dispersive spectrometer (EDS) characterization of the used 4%Ni–V/TiO_2 catalyst revealed that no coke deposition or chlorine species could be detected on the catalyst surface.

Introduction

Chlorinated volatile organic compounds (CVOCs) discharged into the atmosphere as a result of industrial operations are poisonous pollutants and are very harmful organic contaminants, as they exhibit severe toxicity and bioaccumulative properties (Maupin et al., 2012; Zinovyev et al., 2002; Wang et al., 2014a; Cao et al., 2016; Pitkäaho et al., 2011; Chen et al., 2012; Huang et al., 2014a). Catalytic combustion to CO_x, H_2O, HCl, and Cl_2 is a very promising method of pollutant neutralization because it consumes low energy, has high efficiency and the preferential ability to removal harmful CVOCs (Dai et al., 2016; López-fonseca et al., 2003; Pitkäaho et al., 2013; Wang et al., 2014b). Dichloromethane (DCM) belongs to the family of alkyl chlorides and is often used by researchers as a model molecule to investigate the oxidation activity of various catalysts (Yang et al., 2014; Wang et al., 2015).

Our previous study (Huang et al., 2016) showed that a catalyst based on hollow anatase TiO_2 (TiO_2-HA) nanoparticles had high activity, as it demonstrated 90% DCM conversion at 201°C. However, a large amount of chloromethane was generated as a side-product of this conversion reaction. Additionally, the selectivity of the catalyst to CO_x and HCl was poor at low temperatures. Therefore, recent research has

* *Corresponding author. E-mail:* luhf@zjut.edu.cn. (Hanfeng Lu).

https://doi.org/10.1016/j.jes.2019.04.013
1001-0742 © 2019 The Research Center for Eco-Environmental Sciences, Chinese Academy of Sciences. Published by Elsevier B.V.

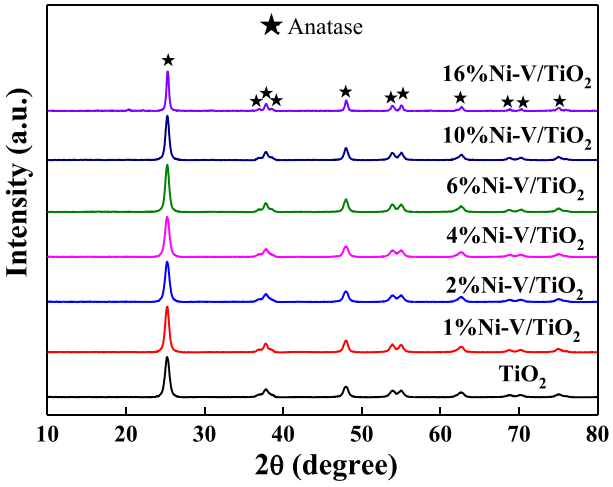

Fig. 1 – X-ray diffraction (XRD) patterns of pure TiO_2 catalyst and Ni–V/TiO_2 series catalysts.

focused on modification of the surface of the hollow TiO_2 structures to enhance its selectivity relative to CO_x and to guarantee its stability at low temperatures (Huang et al., 2016; Chen et al., 2017; Li et al., 2018; Papaefthimiou et al., 1998; Pinard et al., 2004; Scire et al., 2003). Recent studies (Bertinchamps et al., 2006a, 2006b; Shang et al., 2012; Zhang et al., 2015; Huang et al., 2014b) have shown that a favorable interaction exists for Ni-V loading, thereby improving the redox performance of the catalyst and transfer ability of reactive oxygen, and further enhancing the selectivity and stability in the catalytic degradation of CVOCs.

As a continuation of our previous study, this work reports preparation of well-dispersed NiO–VO_x catalysts over pure bulk TiO_2 and over hollow anatase TiO_2 nanoparticles used as a catalyst support (Huang et al., 2016; Zhang et al., 2015). The present work focused on the reduction of the production of the by-product monochloromethane (MCM), improvement of its selectivity for CO_2, and assurance of its stability at low temperatures. The goals of this work were (1) to study the oxidation behavior of DCM over the NiO–VO_x/TiO_2 catalyst relative to pure TiO_2; (2) to clarify the role of NiO–VO_x and (3) to understand the mechanism of catalytic oxidation of DCM and CVOCs in general. The texture, redox behavior and surface acidity of the NiO–VO_x/TiO_2 catalysts (Ni–V/TiO_2), as well as the total oxidation of DCM, were investigated.

1. Materials and methods

1.1. Preparation of the catalysts

1.1.1. Hollow TiO_2 nanoparticles

Anatase nanoparticles with internal cavities were obtained using a cetyltrimethylammonium bromide (CTAB)-assisted hydrothermal method. The starting materials $TiOSO_4{\cdot}2H_2O$ and CTAB were dissolved in 50 mL of deionized (DI) water separately at CTAB/$TiOSO_4$ = 1:12 molar ratio and stirred at 60°C. The $TiOSO_4$ solution was mixed with the CTAB solution and vigorously stirred. The mixture was then kept in a stainless-steel autoclave with 150 mL capacity at 110°C for 24 hr, after which it was cooled to room temperature. The obtained precipitate was filtered, washed multiple times with DI water and ethanol, dried at 110°C and calcined at 500°C for 4 hr in air. Analysis confirmed that the powders were anatase TiO_2 nanoparticles ~11.4 nm in size with symmetrical mesopores 5–25 nm in size and that the particles were homogeneous with a hollow spherical morphology. The specific surface area determined by the Brunauer–Emmett–Teller (BET) method was 94.73 cm^3/g. Details of the characterization methods implemented in this work are described in our previous studies (Huang et al., 2016).

1.1.2. Supported mixed V–Ni oxide catalysts

Catalysts based on mixed V–Ni oxides and supported on TiO_2 were prepared using a conventional citrate sol–gel method. NH_4VO_3 and $Ni(NO_3)_2{\cdot}6H_2O$ with V/Ni = 1:1 molar ratio were dissolved in DI water at 70°C. TiO_2 was then added to the solution. After several minutes, citric acid and carbowax (citric acid / (V + Ni) = 2:1, molar ratio; carbowax/citric acid = 10 wt.%) was added, after which the solution was heated at 80°C under constant stirring until a viscous gel was obtained. All processes above were performed under constant vigorous stirring. The concentrations of vanadium and nickel nitrates as well as the amount of citrate solution were adjusted to obtain catalysts with 1–16 wt.% of vanadium–nickel oxide. The resulting gel was dried at 110°C overnight and then calcined in air at 500°C for 4 hr. The catalysts were marked as m%Ni–V/TiO_2 (m = 1, 2, 4, 6, 10, 16).

1.2. Catalyst characterization

Powder XRD patterns were determined by a diffractometer (X' Pert Pro, PANalytical, Netherlands) with nickel-filtered Cu Kα

Table 1 – Physical properties and XRD data of pure TiO_2 catalyst and Ni–V/TiO_2 catalysts.

Catalyst	S_{BET} (m^2/g)	V_{pore} (cm^3/g)	D_{pore} (nm)	Lattice constant (nm)	Average crystallite size (Å)	T_{50} (°C)	T_{90} (°C)
TiO_2	94.73	0.31	12.98	3.7879	114	175	201
1%Ni-V/TiO_2	90.03	0.30	13.14	3.7891	130	178	212
2%Ni-V/TiO_2	86.90	0.29	13.31	3.7897	132	174	209
4%Ni-V/TiO_2	81.85	0.30	14.39	3.7879	132	168	203
6%Ni-V/TiO_2	77.19	0.28	15.47	3.7875	139	201	235
10%Ni-V/TiO_2	68.72	0.25	17.57	3.7879	148	197	251
16%Ni-V/TiO_2	53.22	0.22	19.19	3.7864	230	212	309

S_{BET}: specific surface area; V_{pore}: average pore volume; D_{pore}: average pore size; T_{50}: temperature when 50% conversion are obtained; T_{90}: temperature when 90% conversion are obtained.

radiation and were recorded at 0.04° intervals in the range of $10° \leq 2\theta \leq 80°$ at a voltage of 45 kV and current of 30 mA. Crystal sizes were obtained using the Scherrer equation. Transmission electron microscopy (TEM) was performed using a microscope (Tecnai G2F30, FEI, Netherland). Samples for TEM analysis were dispersed in absolute alcohol and placed on a copper grid. Specific BET surface areas and porosity were obtained from nitrogen adsorption and desorption isotherms collected at −196°C using a instrument (ASAP 2010, Micromeritics, USA) in static mode. Prior to the measurements, samples were kept in vacuum at 250°C for 3 hr. H_2 temperature-programmed reduction (H_2-TPR) was analyzed using a instrument (FINESORB-3010E, Fantai, China), for which 100 mg of sample was heated in 10 vol.% H_2/Ar flow at 30 mL/min at a 10°C/min heating rate. All samples were heated under highly pure Ar flow at 200°C for 1 hr and then cooled to 50°C prior to the analysis. Surface acidity was determined by adsorption of pyridine, which was quantified by Fourier transform infrared spectroscopy (FTIR) (performed using a spectrometer (Vertex70, Bruker, Germany) equipped with an mercury cadmium telluride (MCT) detector with a scan rate of 32 scans/sec and 2.5 cm^{-1} resolution). Powders were pressed into ~20 mg disks 13 mm diameter, which were pretreated at 400°C for 30 min to avoid catalyst reduction at high temperatures. Spectra were recorded after the samples were cooled to room temperature. Then, 5 μL of pyridine was introduced into the FTIR chamber containing the catalyst, which was allowed to equilibrate for 30 min. FTIR curves were recorded after evacuation for 30 min at 30, 200, and 400°C. Quantities of Brønsted and Lewis sites were assessed by integrating their corresponding peak areas at 1537 and 1446 cm^{-1}, which are attributed to the pyridine adsorbed on Brønsted and Lewis sites (Bertinchamps et al., 2006a; Emeis, 1993), respectively. Thermogravimetric analysis (TGA) was performed using a instrument (STA409PC, NETSCH, Germany) to verify the absence of coke on the catalyst surface. TGA curves of Ni–V/TiO_2 samples were recorded on heating up to 1200°C at a 10°C/min heating rate under N_2/O_2 flow.

1.3. Analysis of catalytic activity

Catalytic performance tests were performed at ambient pressure using a traditional fixed-bed tubular quartz reactor with inner diameter equal to 6 mm. A sandwich structure consisting of quartz sand/catalyst/quartz sand was placed in the middle of the reactor. This sandwich contained 200 mg of the catalyst and ~1800 mg of quartz sand. DCM feed gas was generated by bubbling synthetic air (consisting of 20.8% O_2 and 79.2% N_2) through a saturator containing DCM and cooled in an ice bath. Bypass air flow was used to equilibrate the flow and to provide the desired gas hourly space velocity (GHSV) in the catalyst bed. The flow of the feed gas was 50 mL/min, 1000 ppmV of which was DCM. Total GHSV was 15,000 mL/(hr·g_{cat}). The effluent gases were continuously analyzed using a gas chromatograph (GC-6890N, Agilent, USA) coupled with flame ionization detector (FID) detector and an FTIR spectrometer. Gas chromatography–mass spectrometry (6890N-5975C, Agilent, USA) confirmed formation of by-products. Cl_2 and HCl gases were collected by bubbling the effluent through 0.0125 mol/L NaOH solution (Wu et al., 2012).

2. Results and discussion

2.1. Catalyst characterization

2.1.1. Structure and texture

The XRD patterns and crystal sizes of Ni–V/TiO_2 catalysts with different loadings are presented in Fig. 1 and Table 1. Almost all Ni–V/TiO_2 samples demonstrated peaks characteristic of

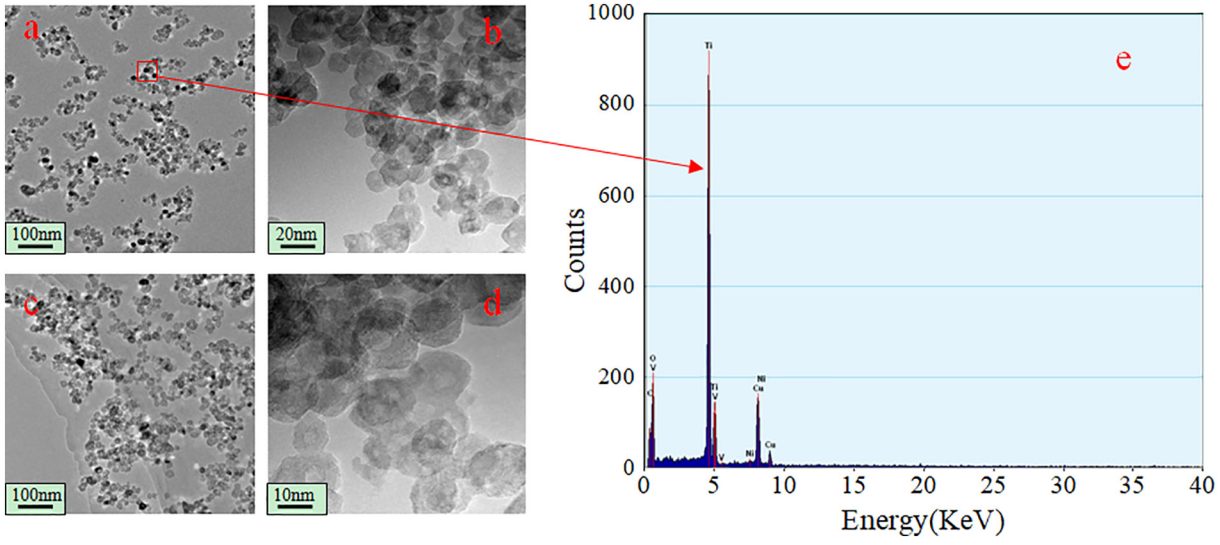

Fig. 2 – Transmission electron microscopy and high resolution transmission electron microscopy images of (a, b) 4%Ni–V/TiO_2 catalyst and (c, d) pure TiO_2 catalyst, and (e) energy dispersive spectrometer spectrum of the indicated area of 4%Ni–V/TiO_2 catalyst.

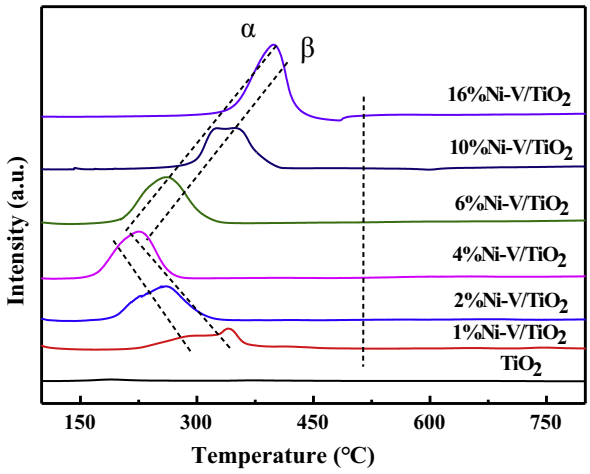

Fig. 3 – H_2 temperature-programmed reduction patterns of pure TiO_2 catalyst and the Ni–V/TiO_2 series catalysts. α and β refer to the NiO and V^{5+} species reduction peak, respectively.

anatase (PDF#21-1272). No other diffraction peaks were detected. These results indicate the presence of stable crystalline phases. No crystalline phases that could be ascribed to VO_x or NiO were indicated. No evidence of anatase structure collapse was observed, suggesting excellent dispersion of vanadium and nickel oxides on the TiO_2 surface. We believe that vanadium and nickel oxide formed either amorphous or solid-solution phases (Bertinchamps et al., 2006b; Wu et al., 2012). The main anatase peak at (101) did not shift to lower or higher angle, indicating that the Ni–V did not distort the TiO_2 lattice or affect its crystallization by forming solid solutions. Therefore, we believe that the Ni and V oxides were anchored only on the surface titanium atoms. The average particle diameters obtained from the (101) XRD peak by the Scherrer equation are shown in Table 1.

The texture of the catalysts was investigated by N_2 adsorption/desorption isotherms. As shown in Table 1, the average crystallite diameter of Ni–V/TiO_2 catalysts increased gradually with increased NiO–VO_x loading. Relative to that of TiO_2, the specific surface area of the Ni–V/ TiO_2 catalysts with different loadings was decreased. A significant increase in crystallite size was observed from 11.4 nm for pure TiO_2 to 23 nm for 16%Ni–V/TiO_2, with a decrease in surface area from 94.73 to 53.22 m^2/g.

Representative TEM patterns were obtained to analyze the morphology and dispersion changes of the TiO_2-HA catalysts loaded with active Ni–V components. TEM, high resolution transmission electron microscope (HRTEM), and EDS (energy dispersive spectrometer) spectra of 4%Ni–V/TiO_2 and hollow TiO_2 catalysts are shown in Fig. 2. According to the EDS spectra (Fig. 2e), the peaks assigned to Ni and V found in the spectra indicate the presence of certain amounts of Ni and V elements, which further indicates that the Ni–V active components are effectively loaded on the surface of the TiO_2–HA catalyst. By comparison of TEM and HRTEM images (Fig. 2a–d), no significant change of morphology was observed between the Ni–V modified catalyst and the pure TiO_2-HA catalyst. The Ni–V/TiO_2 catalyst still possessed good dispersion, and the HRTEM image shows that it retained the hollow spherical morphology.

2.1.2. Redox properties of the catalysts

H_2-TPR analysis was used to study the reducibility of the TiO_2-based catalysts in the 100–800°C temperature range. H_2-TPR profiles of pure TiO_2 and modified TiO_2 catalysts are shown in Fig. 3. The Ni–V/TiO_2 catalysts mainly exhibited two partially overlapped reduction peaks (α and β peaks) below 500°C, respectively. The pure TiO_2 catalyst showed reduction above 540°C, and these experimental results also indicate that no reduction peak of the pure TiO_2 catalyst occurred in this temperature range (Wu et al., 2012). Thus, the two reduction peaks below 500°C can be attributed to the reduction of the surface species resulting from NiO (α peak) interacting with V^{5+} species (β peak) (Vislovskiy et al., 2003). For the Ni–V/TiO_2 catalysts, with the incorporation of Ni–V species, the intensities of the two reduction peaks increased, the α peak temperature shifted from 297 to 207°C, and the β peak temperature decreased from 355 to 235°C when the Ni–V loading reached 4 wt.%, which indicates that the active component particles exposed on the surface of the TiO_2 are constantly increasing. With continuously increased loading up to 16 wt.%, the intensities of the reduction peaks persistently enhanced and the temperature of the reduction peaks constantly increased. This may be due to the fact that the vanadium and nickel active component loadings are higher than their dispersion threshold, resulting in the aggregation of oxides on the surface of TiO_2 and formation of a microcrystalline structure. The 4%Ni–V/TiO_2 sample exhibited the lowest α and β reduction peak temperatures, approximately 207 and 235°C, respectively, indicating that the lattice oxygen of NiO-VO_x reduced more easily. The low-temperature peak area indicates that the 4%Ni–V/TiO_2 catalyst has a high concentration of oxygen vacancies as well as surface-adsorbed oxygen. The temperatures of the α or β reduction peaks varied in increasing order as follows: 4%Ni–V/TiO_2 < 2%Ni–V/TiO_2 < 1%Ni–V/TiO_2 < 6%Ni–V/TiO_2 < 10%Ni–V/TiO_2 < 16%Ni–V/TiO_2. According to the results, the loading of vanadium and nickel oxide on the TiO_2 surface effectively solves the problem of the lack of redox performance of the pure TiO_2 catalyst. Therefore, interaction between NiO and VO_x increases the quantity of NiO and V^{5+} pairs, exhibiting stronger oxidation ability and oxygen species in the modified TiO_2 catalysts. These properties would be very beneficial for the destruction of CVOCs and their intermediate by-products, considering that the catalytic activities of all investigated samples agree with their redox properties. An appropriate amount of Ni–V loading on the TiO_2 surface can promote some synergy between the active components and the carrier, as well as accelerate the mobility of surface-active oxygen species to some extent, to improve the catalytic degradation performance and product selectivity of DCM by the catalyst.

2.1.3. Acidic properties of the catalysts

The catalytic combustion activity in relationship to DCM is considered to be related to the synergy between the catalyst's

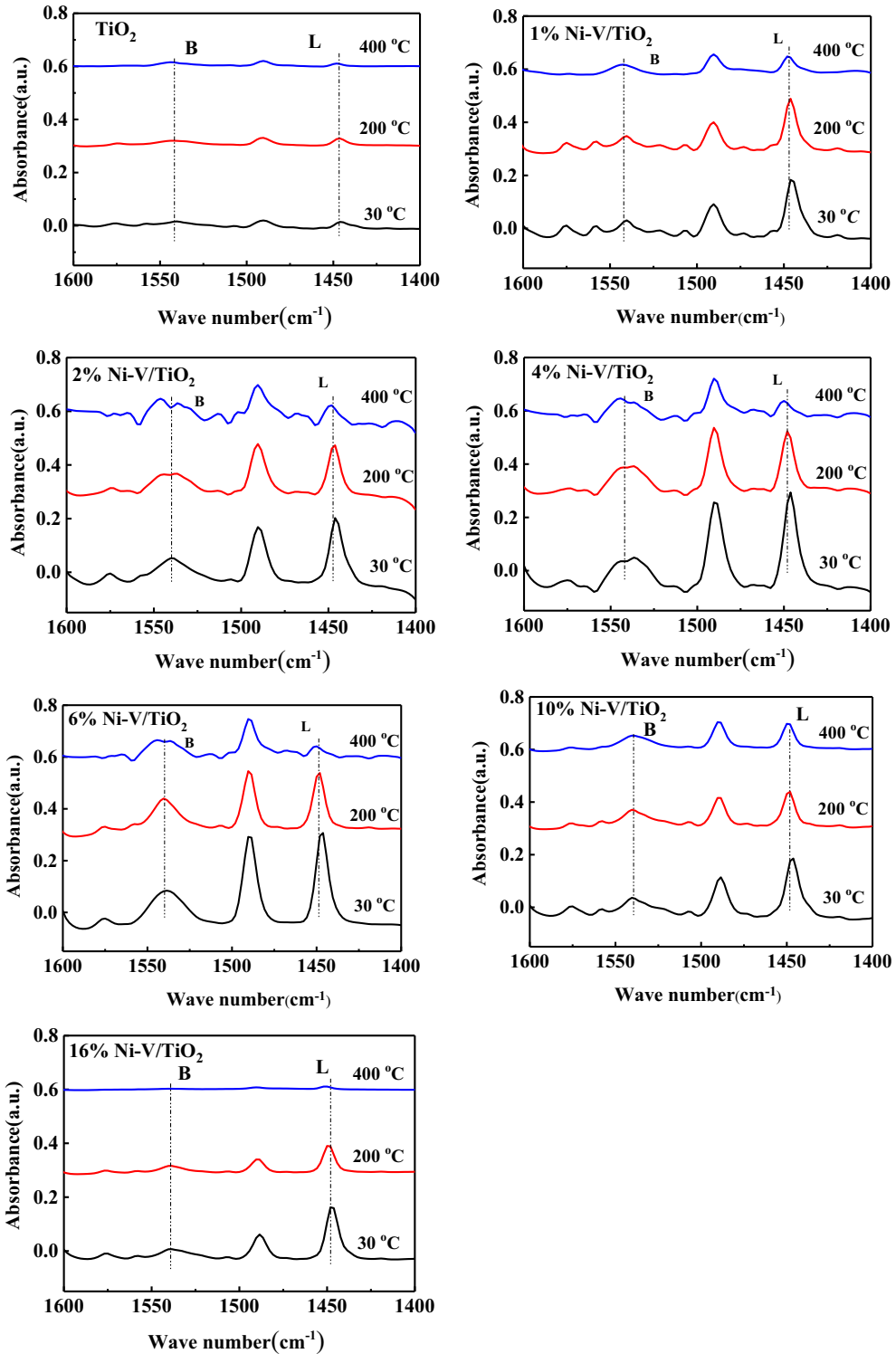

Fig. 4 – Pyridine adsorption-temperature programmed desorption Fourier transform infrared spectroscopy (FTIR) for pure TiO_2 and the Ni–V/TiO_2 series catalysts. B and L in the figure refer to Brønsted and Lewis sites, respectively.

acidity and its oxidation action. Acidity helps activate C–Cl bonds. We used FTIR-pyridine to characterize the acidity on the catalyst surfaces (shown in Fig. 4). Spectra were collected after evacuation at 30, 200, and 400°C. Spectra collected after these treatments corresponded to sites associated with groups with weak, medium, and strong acidity, respectively (Kang et al., 2002). Fig. 4 presents the FTIR-pyridine of Ni–V/TiO_2 catalysts with different Ni–V loadings. Brønsted (B sites) and Lewis sites (L sites) were determined by integrating the peak areas at 1537 and 1446 cm^{-1}, which correspond to pyridine species adsorbed on B and L sites, respectively (Zhang et al., 2015; Futamura et al., 2002). Pyridine adsorbed

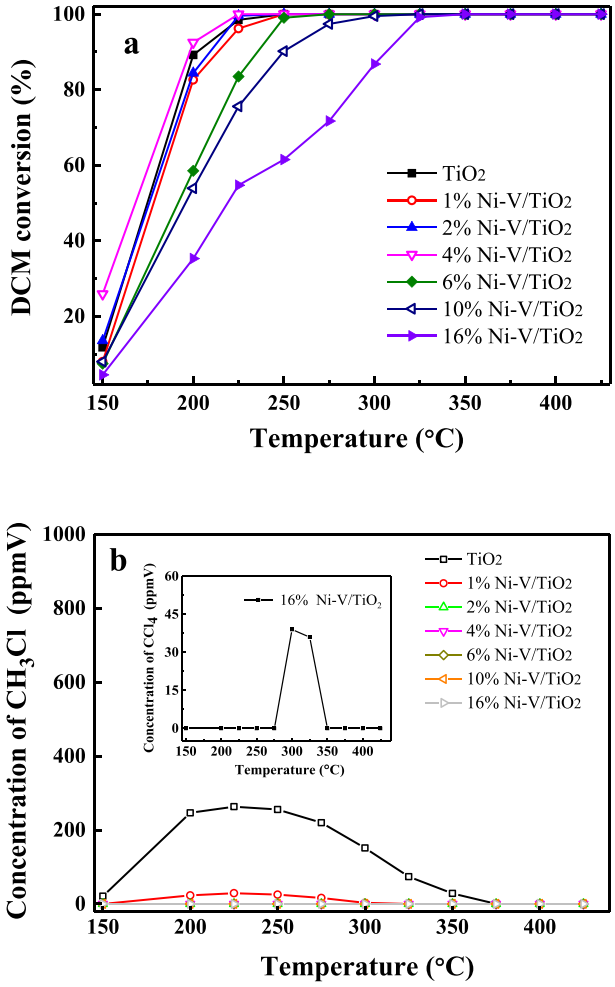

Fig. 5 – (a) Conversion curve of dichloromethane (DCM), (b) concentration of byproduct CH_3Cl, and (inset) concentration of byproduct CCl_4 during DCM combustion over pure TiO_2 and Ni–V/TiO_2 series catalysts. Combustion conditions: gas composition 1000 ppmV DCM in air and gas hourly space velocity (GHSV) 15,000 mL/(hr·g_{cat}).

on the weakly acidic sites was easily desorbed with increasing temperature. The loading of Ni–V active components was found to significantly increase the number of B and L sites on the modified catalyst surface compared to the pure TiO_2 catalyst, which corresponds with the conclusion derived from the literature that VO_x species can improve the strength and increase the number of B sites of the TiO_2 surface. In addition, all the modified TiO_2 catalysts possessed a certain number of moderately strong acidic sites, including B and L acidic sites. Temperature increase significantly decreased the amount of adsorbed pyridine on the L sites of all TiO_2-supported catalysts. Thus, L sites on all these catalysts were mainly weak L sites. With increased active component loading, the peak area corresponding to the B acidic sites increased sharply relative to L acidic sites; and the moderately strong and strong acidic sites also increased until a plateau was reached, where the Ni–V loading reached 4 wt.%. At more than 4 wt.% loading, the peak areas decreased continuously, regardless of whether the peaks belonged to L or B acidic sites. When the Ni–V loading reached 16 wt.%, the areas of the peaks at 1537 and 1446 cm^{-1} were smaller than that for 1%Ni–V loading. The 16%Ni–V/TiO_2 catalyst was found to contain no moderately strong B sites, and no peaks were observed at 400°C, which indicated that the catalyst had no strong sites. Both B and L acidic sites play a very important role in the oxidative neutralization of harmful CVOCs. These results reveal that 4%Ni–V/TiO_2 possesses a maximum number of acidic and moderately strong acidic sites, which can provide abundant surface hydroxyl groups. The surface hydroxyl groups can activate CVOC molecules to further improve their catalytic performance.

2.2. Catalytic performance evaluation

2.2.1. Catalytic activity measurement

Fig. 5a shows DCM light-off curves for different Ni–V/TiO_2 catalysts. A noticeable change in catalytic activity can be observed for both pure TiO_2 and Ni–V/TiO_2 catalysts with different loadings by comparing their T_{90} values (which are indicative of the reaction temperature required to reach 90% conversion). The sequence of the catalytic activity for DCM combustion is as follows: TiO_2 (201°C) > 4% Ni–V/TiO_2 (203°C) > 2% Ni–V/TiO_2 (209°C) > 1% Ni–V/TiO_2 (212°C) > 6% Ni–V/TiO_2 (235°C) > 10% Ni–V/TiO_2 (251°C) > 16% Ni–V/TiO_2 (309°C). The 4%Ni–V/TiO_2 catalyst exhibited nearly the same catalytic activity as TiO_2-HA (T_{90} is 201°C); thus, the loading of active components did not promote the catalytic performance of DCM degradation notably. Moreover, the Ni–V/TiO_2 catalysts were found to exhibit enhanced conversion with increased NiO–VO_x loading from 1% to 4%, the 4% Ni–V/TiO_2 catalyst demonstrated the highest activity, and the T_{90} value was only 203°C. However, with further increase of the NiO–VO_x loading to 6%, the Ni–V/TiO_2 catalysts demonstrated declined catalytic activity (T_{90} value reached 235°C), and when the loading increased to 16%, the T_{90} was 309°C, relative to 4% loading, an increase of nearly 110°C. This may be due to the fact that the increase of active components may destroy the surface texture of TiO_2, which restrains the catalytic activity of DCM destruction. Determining if any by-products harmful to human health are formed during the DCM combustion reaction is important. Thus, the distribution of by-products was measured and displayed in Fig. 5b. As shown in Fig. 5b, MCM is the only organic by-product detected in the waste stream during DCM decomposition. Interestingly, the amount of MCM, which was copiously generated in DCM conversion over the pure TiO_2 catalyst, sharply decreased with the Ni–V supported catalysts, but the catalytic performance did not increase. No CH_3Cl was detected for the *m*%Ni–V/TiO_2 (*m* = 2, 4, 6, 10, and 16) catalysts, indicating that further rupture of C–Cl bonds occurs when the V–Ni loadings reached 2%. Notably, at higher temperature, another Cl-containing organic compound was traced in DCM decomposition over the 16% Ni–V/TiO_2 catalyst, and the catalytic activity was 80%; thus, DCM degradation may exhibit a different reaction pathway, such as a chlorination reaction, with other catalysts. Other studies in the literature have reported that in the presence of Cl species, the reactant decomposition results in the information of polychlorinated by-products over the metal oxide catalyst at higher temperature through a chlorination reaction (Gu et al., 2010).

The TPR results revealed that the 4%Ni–V/TiO_2 catalyst had the lowest temperature reduction peak, at which the lattice oxygen of NiO–VO_x mixed oxide reduced easily. It also showed a

larger reduction peak area, which indicates that it also has higher concentrations of oxygen vacancies and adsorbed oxygen. The FTIR spectra of pyridine adsorption show that 4% Ni–V/TiO_2 possesses high surface acidity and more moderately strong acidic sites, especially the B acidic sites, which results in better catalytic activity, while the 16%Ni–V/TiO_2 catalyst, which, possessed fewer acid sites and did not have any of the strongest acidic sites, exhibited the worst catalytic activity. These observations are indicative of a relationship between the number of acidic sites on the catalyst surface and overall catalytic activity. In general, the more acidic sites exposed on the catalyst surface, the more enhanced the catalytic performance is. High content of NiO–VO_x in the samples (such as 16%Ni–V/TiO_2) can lead to the blockage of TiO_2 active sites by NiO–VO_x, significantly inhibiting the overall catalytic activity. The significantly lower surface area of the catalysts with high NiO–VO_x contents in comparison to the catalysts with lower NiO–VO_x contents proves this observation. For example, the surface area of 16%Ni–V/TiO_2 was 53.22 m^2/g, which is considerably lower than the surface area of unmodified TiO_2 (which is equal to 94.73 m^2/g). Comparison of these surface area values indicates blockage of active sites by excess NiO–VO_x. Thus, the enhanced DCM and MCM conversion activity observed for the 4%Ni–V/TiO_2 catalyst can be attributed to the acidity and redox properties of the catalyst surface. A similar conclusion was obtained for the oxidation of 1,2-dichloroethane (DCE) using CeO_2-modified ultra-stable Y (USY) zeolites, and, as the authors indicated, both the acidity and redox properties played important roles during this process. T_{90}, surface acidity, and redox property results of the Ni–V/TiO_2 catalysts reveal that the catalytic behaviors of the catalyst correlate with the simultaneous contributions of surface acidity and redox properties. The 4%Ni–V/TiO_2 sample with the optimal combination (both high reducibility and high surface acidity) was more active.

2.2.2. Durability test

Generally, the formation of HCl and/or Cl_2 from the catalytic oxidation of CVOCs deactivates catalysts, particularly noble metal catalysts. Our previous works showed that this deactivation was the most challenging obstacle for the combustion of CVOCs over TiO_2-based catalysts (Huang et al., 2016). Therefore, in this work we performed stability tests using the 4%Ni–V/TiO_2 sample. A stream containing 1000 ppmV of the reactant in air at 225°C was passed over the catalyst at 15,000 mL/(hr·g_{cat}) space velocity. The stability of the pure TiO_2 catalyst is exhibited in the inset in Fig. 6. The unmodified TiO_2 catalyst demonstrated rapid deactivation during the first 150 min at 200°C. During this time, DCM conversion was constant (90%) for the first 90 min (90%) but decreased to 61% over the next 30 min. By contrast, over the 4%Ni–V/TiO_2 catalyst, conversion of DCM barely decreased during the initial 2 hr and maintained a constant value above 95% during the whole test duration of 98 hr, which agrees with the activity test results. No MCM was detected. Thus, addition of Ni–V improved the catalytic performance and stability of TiO_2 for catalytic DCM combustion.

Typically, deactivation of noble or transition metal catalysts during catalytic combustion of CVOCs is attributed to chlorination of the active material, adsorption of inorganic chlorine species and/or formation of coke deposits on

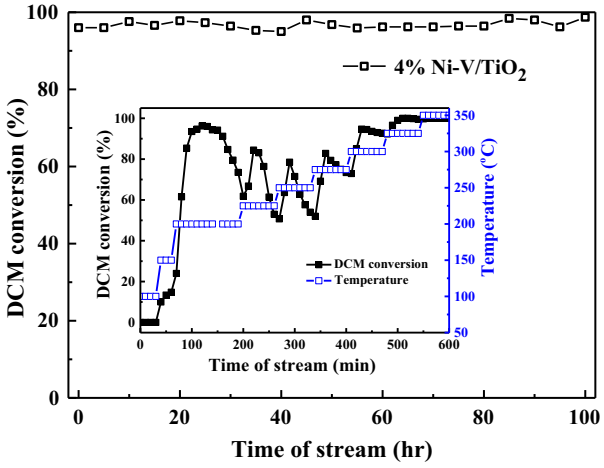

Fig. 6 – Stability of 4%Ni–V/TiO_2 and (inset) pure TiO_2 catalysts in the DCM oxidation. Combustion conditions: gas composition 1000 ppmV DCM in air, temperature 225°C and GHSV 15,000 mL/(hr·g_{cat}).

active sites. Furthermore, chlorinated species (like $MOCl_x$ or MCl_x) actively participate in the formation of chlorohydrocarbon by-products, especially if HCl or Cl_2 is present (Ran et al., 2013, 2014; Yang et al., 2015a; Cen et al., 2014). Thus, active-phase stabilization and rapid removal of unwanted HCl from the active catalytic sites are essential for enhancing catalyst stability. Addition of NiO–VO_x can improve the chlorination resistance of TiO_2 because of its extraordinary stability (such as limited reaction with Cl-species and resistance when exposed to HCl) and enable easier removal of HCl. Additionally, HCl is the main product formed when the 4%Ni–V/TiO_2 catalyst is used, mostly because of the acidic sites that translate into abundant surface hydroxyl groups. Therefore, the 4%Ni–V/TiO_2 catalyst demonstrated excellent low-temperature stability relative to DCM, without any deactivation.

2.2.3. Characterization of the used catalyst

As previously mentioned, coke deposition on the catalyst surface deactivates the overall oxidation reaction, reducing the amount of neutralized chlorinated hydrocarbons. This occurs because of the formation of carbonaceous deposits inside the mesopores and coke growth on the external surfaces of the crystal, which physically block the pores and active sites on the catalytic surface. Therefore, to investigate coke formation and deposition during 100 hr-long stability testing, O_2-TG analysis of fresh and used 4%Ni–V/TiO_2 catalysts was performed. As shown in Fig. 7, both catalysts exhibited weight loss phenomena at three stages. Generally, the catalyst weight loss at low temperature (less than 250°C) can be attributed to the removal of physically adsorbed material on the surface (such as H_2O or DCM). The used catalyst exhibited a larger weight loss than the fresh catalyst because, in the DCM atmosphere, the former adsorbed a certain amount of DCM when the durability test temperature decreased from 225°C to room temperature. Thus, when the TG temperature was increased to 250°C, this resulted in the complete oxidation of the weakly

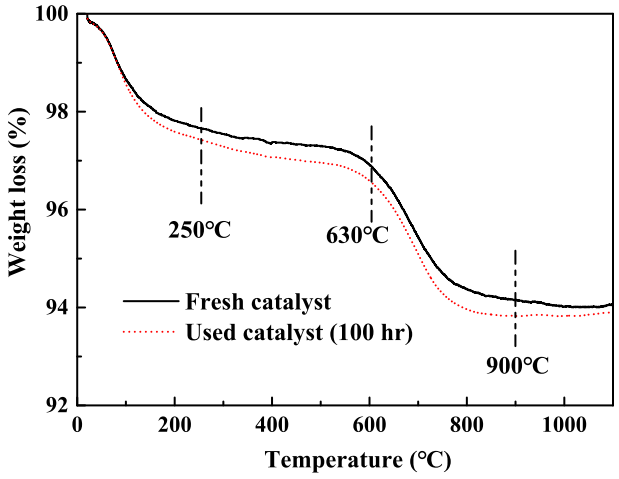

Fig. 7 – Thermogravimetric analysis of fresh and used 4% Ni–V/TiO_2 catalysts for catalytic DCM combustion.

and strongly adsorbed DCM molecules due to the high catalytic activity. According to the literature, within the temperature range of 250–630°C, the weight loss of a catalyst may be related to the combustion of coke deposits and the oxidation of chemically adsorbed chlorine species on the catalyst surface (Yang et al., 2015b). We found that the used catalyst showed virtually the same weight loss as the fresh catalyst at this temperature, which confirmed that no coke formed and deposited on the 4%Ni–V/TiO_2 catalyst in the total oxidation of DCM after the 100 hr durability test. The weight loss at the third stage is possibly attributed to the volatilization of V species, in which V_2O_5 exists at a molten state at high temperature and significantly evaporates when the temperature rises continuously (approximately 700°C); and the vapor pressure increases with increased temperature (Pitkäaho et al., 2012a, 2012b).

To study chlorine species decomposition on the catalyst surface, EDS analysis of fresh and used catalysts was performed. Qualitative analysis was carried out due to the restricted experimental conditions. Results showed no visible EDS peaks related to Cl species for both fresh and used catalysts. These results indicate that no Cl-deposition occurred on the surface of the used catalyst, very likely because of the NiO–VO_x presence, which effectively removes Cl species.

Characterization of the used 4%Ni–V/TiO_2 catalyst indicated that no coke deposition or chlorine species formation occurred on the catalyst surface, which is related to the large number of active oxygen species and their mobility as well as abundant acidic and moderately strong acidic sites. Thus, 4% Ni–V/TiO_2 has great catalytic activity and excellent stability for DCM at lower temperatures.

2.3. *Mechanism of DCM degradation using Ni–V/TiO_2 catalyst*

Based on the literature, a detailed potential decomposition mechanism of DCM oxidation over Ni–V/TiO_2 was proposed (Fig. 8) (Ran et al., 2013, 2014; Yang et al., 2015a, 2015b; Van den Brink et al., 1998, 1999; Seo et al., 2013; Aouad et al., 2007; Guo et al., 2013; Xia et al., 2017; Lin et al., 2012). (1) The first stage is very likely the dissociative adsorption of C–Cl groups on acid sites through the Cl abstraction mechanism. CH_2Cl_2 molecules can chemisorb on one Ti-OH site, which acts as an acidic site to form Ti-OCH_2Cl and inorganic chlorine. (2) Chlorine formed after the breakage of the C–Cl bonds either combines with a proton, forming a gaseous HCl molecule (which is then released), or resorbs at the surface of the catalyst and blocks the active site. (3) The active oxygen species directly participate in the oxidation of DCM and its intermediate products (such as adsorbed formaldehyde or CO), forming gas-phase reaction products (CO_x, H_2O, and HCl). (4) The gas-phase oxygen binds to the surface to replenish the oxygen consumed. Considering the mobility of active oxygen species, Cl-species adsorbed on

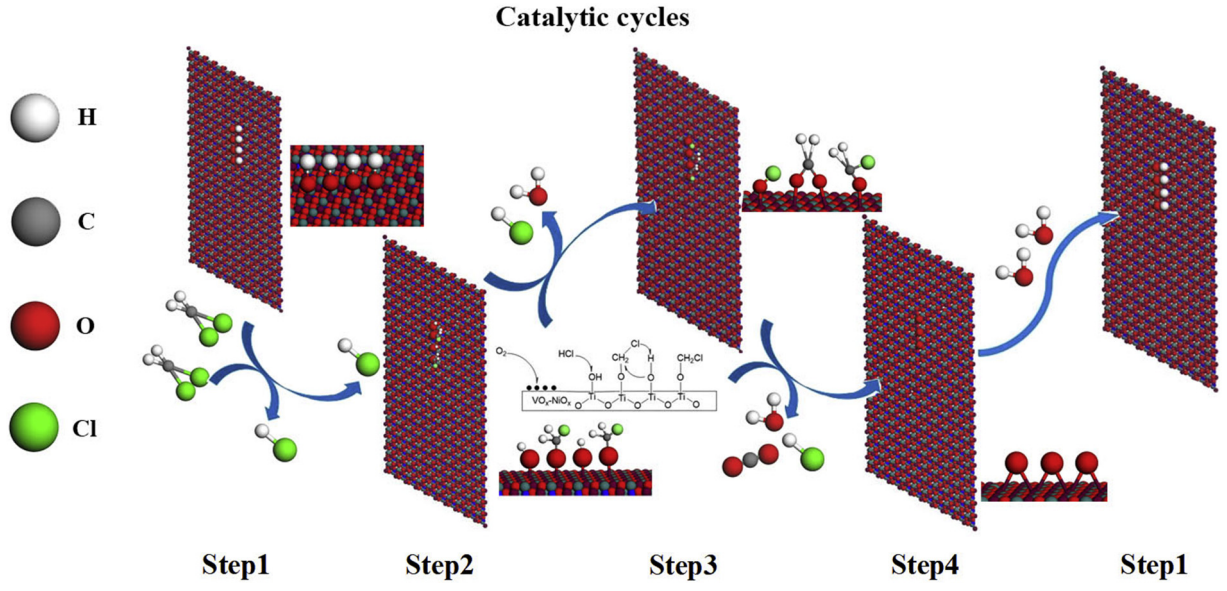

Fig. 8 – Possible decomposition mechanism of DCM oxidation over Ni–V/TiO_2 catalyst.

active sites can be transferred to the oxygen vacancies on the NiO–VO_x surface and react with numerous surface hydroxyl groups to form HCl under an oxygen-rich atmosphere, which is responsible for the stability of 4%Ni–V/TiO_2. (5) The dissociation of water from DCM oxidation benefits the opening of titanium Ti-O-Ti bridges, which increases the number of hydroxyl groups on the surface until the consumed OH groups are replenished. The weak redox properties of pure TiO_2 are such that the intermediate formaldehyde species cannot be oxidized immediately, so that CH_3Cl formation occurs because of the transfer of a formaldehyde hydride from the surface to a Ti-OCH_2Cl molecule.

3. Conclusions

Our experimental results showed that the addition of NiO–VO_x significantly improved the stability of TiO_2 and inhibited formation of MCM by-products. Among the series of Ni–V/TiO_2 catalysts, 4%Ni–V/TiO_2 possesses the highest catalytic activity, with T_{90} at only 203°C. No by-products and no significant changes in catalytic activity were observed after combusting DCM in a 100 hr continuous stability test. Furthermore, O_2-TG and EDS characterization of the used 4%Ni–V/TiO_2 catalyst revealed that no coke deposition or chlorine species occurred on the catalyst surface. This work demonstrates that Ni–V/TiO_2 is highly active for DCM oxidation and possess excellent stability; therefore, it has promising potential in practical application.

Acknowledgments

This work was supported by the National Natural Science Foundation of China (Nos. 21506194 and 21676255), the Provincial Natural Science Foundation of Zhejiang Province (No. Y16B070025), and the Commission of Science and Technology of Zhejiang Province (Nos. 2017C03007 and 2017C33106).

REFERENCES

Aouad, S., Saab, E., Abi-Aad, E., Aboukais, A., 2007. Study of the Ru/Ce system in the oxidation of carbon black and volatile organic compounds. Kinet. Catal. 48, 835–840.

Bertinchamps, F., Gregoire, C., Gaigneaux, E., 2006a. Systematic investigation of supported transition metal oxide based formulations for the catalytic oxidative elimination of (chloro)-aromatics: Part I: Identification of the optimal main active phases and supports. Appl. Catal. B 66, 1–9.

Bertinchamps, F., Gregoire, C., Gaigneaux, E., 2006b. Systematic investigation of supported transition metal oxide based formulations for the catalytic oxidative elimination of (chloro)-aromatics: Part II: Influence of the nature and addition protocol of secondary phases to VOx/TiO_2. Appl. Catal. B 66, 10–22.

Cao, S., Wang, H.Q., Yu, F.X., Shi, M.P., Chen, S., Weng, X.L., 2016. Catalyst performance and mechanism of catalytic combustion of dichloromethane (CH_2Cl_2) over Ce doped TiO_2. J. Colloid Interface Sci. 463, 233–241.

Cen, W.L., Liu, Y., Wu, Z.B., Liu, J., Wang, H.Q., Weng, X.L., 2014. Cl species transformation on CeO_2(111) surface and its effects on CVOCs catalytic abatement: a first-principles investigation. J. Phys. Chem. C 118, 6758–6766.

Chen, Q.Y., Li, N., Luo, M.F., Lu, J.Q., 2012. Catalytic oxidation of dichloromethane over Pt/CeO_2–Al_2O_3 catalysts. Appl. Catal. B 127, 159–166.

Chen, X., Xu, Q.Q., Zhou, Y., Zhu, Q.L., Huang, H.F., Pan, Z.Y., 2017. Facile and flexible preparation of highly active CuCe monolithic catalysts for VOCs combustion. Chemistry Select 2, 9069–9073.

Dai, Q.G., Yin, L.L., Bai, S.X., Wang, W., Wang, X.Y., Gong, X.Q., 2016. Catalytic total oxidation of 1,2-dichloroethane over VO_x/CeO_2 catalysts: further insights via isotopic tracer techniques. Appl. Catal. B 182, 598–610.

Emeis, C.A., 1993. Determination of integrated molar extinction coefficients for infrared absorption bands of pyridine adsorbed on solid acid catalysts. J. Catal. 141, 347–354.

Futamura, S., Zhang, A.H., Einaga, H., 2002. Involvement of catalyst materials in nonthermal plasma chemical processing of hazardous air pollutants. Catal. Today 72, 259–265.

Gu, Y.L., Yang, Y.X., Qiu, Y.M., Sun, K.P., Xu, X.L., 2010. Combustion of dichloromethane using copper–manganese oxides supported on zirconium modified titanium–aluminum catalysts. Catal. Commun. 12, 277–281.

Guo, M.C., Li, L.P., Lin, H.F., Zuo, Y., Huang, X.S., Li, G.S., 2013. Targeted deposition of ZnO_2 on brookite TiO_2 nanorods towards high photocatalytic activity. Chem. Commun. 49, 11752–11754.

Huang, H., Dai, Q.G., Wang, X.Y., 2014a. Morphology effect of Ru/CeO_2 catalysts for the catalytic combustion of chlorobenzene. Appl. Catal. B 158–159, 96–105.

Huang, H.F., Ning, X.J., Jiang, X.J., Gu, L., Lu, H.F., 2014b. Catalytic combustion of chlorinated volatile organic compounds over V-M/TiO_2 (M=Cu, Cr, Ce, Mn, Mo) catalysts. China Environ. Sci. 34, 2179–2185.

Huang, H.F., Zhang, X.X., Jiang, X.J., Dou, K., Ni, Z.Y., Lu, H.F., 2016. Hollow anatase TiO_2 nanoparticles with excellent catalytic activity for dichloromethane combustion. RSC Adv. 6, 61610–61614.

Kang, M., Kim, B.J., Cho, S.M., 2002. Decomposition of toluene using an atmospheric pressure plasma/TiO_2 catalytic system. Mol. Catal. A: Chem. 180, 125–132.

Li, H., Wang, Y., Chen, X., Liu, S., Zhou, Y., Zhu, Q.L., 2018. Preparation of metallic monolithic Pt/FeCrAl fiber catalyst by suspension spraying for VOCs combustion. RSC Adv. 8, 14806–14811.

Lin, H.F., Li, L.P., Zhao, M.L., Huang, X.S., Chen, X.M., Li, G.S., 2012. Synthesis of high-quality brookite TiO_2 single-crystalline nanosheets with specific facets exposed: Tuning catalysts from inert to highly reactive. J. Am. Chem. Soc. 134, 8328–8331.

López-fonseca, R., Rivas, B.D., Gutiérrez-ortiz, J.I., Aranzabal, A., González-Velascoet, J.R., 2003. Enhanced activity of zeolites by chemical dealumination for chlorinated VOC abatement. Appl. Catal. B 41, 31–42.

Maupin, I., Pinard, L., Mijoin, J., Magnoux, P., 2012. Bifunctional mechanism of dichloromethane oxidation over Pt/Al_2O_3: CH_2Cl_2 disproportionation over alumina and oxidation over platinum. J. Catal. 291, 104–109.

Papaefthimiou, P., Ioannides, T., Verykios, X.E., 1998. Performance of doped Pt/TiO_2 (W^{6+}) catalysts for combustion of volatile organic compounds (VOCs). Appl. Catal. B 15, 75–92.

Pinard, L., Magnoux, P., Ayrault, P., 2004. Oxidation of chlorinated hydrocarbons over zeolite catalysts 2. Comparative study of dichlorornethane transformation over NaX and NaY zeolites. J. Catal. 221, 662–665.

Pitkäaho, S., Ojala, S., Maunula, T., Savimäki, A., Kinnunen, T., Keiskia, R.L., 2011. Oxidation of dichloromethane and

perchloroethylene as single compounds and in mixtures. Appl. Catal. B 102, 395–403.
Pitkäaho, S., Matejova, L., Ojala, S., Gaalova, J., Keiski, R.L., 2012a. Oxidation of perchloroethylene—activity and selectivity of Pt, Pd, Rh, and V_2O_5 catalysts supported on Al_2O_3, Al_2O_3-TiO_2 and Al_2O_3-CeO_2. Appl. Catal. B 113–114, 150–159.
Pitkäaho, S., Matejova, L., Jiratova, K., Ojala, S., Keiski, R.L., 2012b. Oxidation of perchloroethylene—activity and selectivity of Pt, Pd, Rh, and V_2O_5 catalysts supported on Al_2O_3, Al_2O_3–TiO_2 and Al_2O_3–CeO_2. Part 2. Appl. Catal. B 126, 215–224.
Pitkäaho, S., Nevanperä, T., Matejova, L., Ojala, S., Keiski, R.L., 2013. Oxidation of dichloromethane over Pt, Pd, Rh, and V_2O_5 catalysts supported on Al_2O_3, Al_2O_3–TiO_2 and Al_2O_3–CeO_2. Appl. Catal. B 138–139, 33–42.
Ran, L., Qin, Z., Wang, Z.Y., Wang, X.Y., Dai, Q.G., 2013. Catalytic decomposition of CH_2Cl_2 over supported Ru catalysts. Catal. Commun. 37, 5–8.
Ran, L., Qin, Z., Wang, Z.Y., Wang, X.Y., Dai, Q.G., 2014. The effect of Ce on catalytic decomposition of chlorinated methane over RuOx catalysts. Appl. Catal. A 470, 442–450.
Scire, S., Minico, S., Crisafulli, C., 2003. Pt catalysts supported on H-type zeolites for thecatalytic combustion of chlorobenzene. Appl. Catal. B 45, 117–125.
Seo, Y., Kim, S., Ahn, J., Jeong, I., 2013. Determination of the local symmetry and the multiferroic-ferromagnetic crossover in $Ni_xCo_xV_2O_8$ by using Raman scattering spectroscopy. J. Korean Phys. Soc. 62, 116–120.
Shang, X.S., Hu, G.R., Zhao, J.P., Zhang, F.W., 2012. Regenaration of full-scale commercial honeycomb monolith catalyst (V_2O_5-WO_3/TiO_2) used in coal-fired power plant. J. Ind. Eng. Chem. 18, 3–519.
Van den Brink, R.W., Mulder, P., Louw, R., Sinquin, G., Petit, C., Hindermann, J.P., 1998. Catalytic oxidation of dichloromethane on γ-Al_2O_3: a combined flow and infrared spectroscopic study. J. Catal. 180, 153–160.
Van den Brink, R.W., Mulder, P., Louw, R., 1999. Catalytic combustion of chlorobenzene on Pt/γ-Al_2O_3 in the presence of aliphatic hydrocarbons. Catal. Tody. 54, 101–106.
Vislovskiy, V.P., Shamilov, N.T., Sardarly, A.M., Talyshinskii, R.M., Bychkov, V.Y., Ruizc, P., 2003. Oxidative conversion of isobutane to isobutene over V-Sb-Ni oxide catalysts. Appl. Catal. A 250, 143–150.
Wang, X.Y., Ran, L., Dai, Y., Lu, Y.J., Dai, Q.G., 2014a. Removal of Cl adsorbed on Mn–Ce–La solid solution catalysts during CVOC combustion. J. Colloid Interface Sci. 426, 324–332.
Wang, Y., Liu, H.H., Wang, S.Y., Luo, M.F., Lu, J.Q., 2014b. Remarkable enhancement of dichloromethane oxidation over potassium-promoted Pt/Al_2O_3 catalysts. J. Catal. 311, 314–324.
Wang, Y., Jia, A., Luo, M., Lu, J., 2015. Highly active spinel type $CoCr_2O_4$ catalysts for dichloromethane oxidation. Appl. Catal. B 165, 477–486.
Wu, M., Ung, K.C., Dai, Q.G., Wang, X.Y., 2012. Catalytic combustion of chlorinated VOCs over VOx/TiO_2 catalysts. Catal. Commun. 18, 72–75.
Xia, Z.J., Lu, H.F., Liu, H.Y., Zhang, Z.K., Chen, Y.F., 2017. Cyclohexane dehydrogenation over Ni-Cu/SiO_2 catalyst: effect of copper addition. Catal. Commun. 90, 39–42.
Yang, P., Meng, Z.H., Yang, S.S., Zhou, R.X., 2014. Highly active behaviors of CeO_2-CrOx mixed oxide catalysts in deep oxidation of 1,2-dichloroethane. J. Mol. Catal. A 393, 75–83.
Yang, P., Yang, S.S., Shi, Z.N., Zhou, R.X., 2015a. Deep oxidation of chlorinated VOCs over CeO_2-based transition metal mixed oxide catalysts. Appl. Catal. B 162, 227–235.
Yang, P., Shi, Z.N., Yang, S.S., Zhou, R.X., 2015b. High catalytic performances of CeO_2–CrOx catalysts for chlorinated VOCs elimination. Chem. Eng. Sci. 126, 361–369.
Zhang, X.H., Pei, Y., Ning, X.J., Lu, H.F., Huang, H.F., 2015. Catalytic low-temperature combustion of dichloromethane over V-Ni/TiO_2 catalyst. RSC Adv. 5, 79192–79199.
Zinovyev, S., Perosa, A., Yufit, S., Tundo, P., 2002. Hydrodechlorination and hydrogenation over raney-Ni under multiphase conditions: role of multiphase environment in reaction kinetics and selectivity. J. Catal. 211, 347–354.